Available online at www.sciencedirect.com
SCIENCE DIRECT®
Journal of Photochemistry and Photobiology A: Chemistry 161 (2003) 11–20
Journal of Photochemistry and Photobiology A:Chemistry
www.elsevier.com/locate/jphotochem

A study on characteristics of an electrolytic–photocatalytic reactor using an anode coated with TiO_2

Kwang-Wook Kim [a,*], Eil-Hee Lee [a], Young-Jun Kim [b], Mi-Hye Lee [c], Dong-Woo Shin [d]

[a] *Korea Atomic Energy Research Institute, Yusong, Taejeon, South Korea*
[b] *Department of Chemical Engineering, Hannam University, Taejeon, South Korea*
[c] *Busan Technology Appraisal Center, Korea Technology Credit Guarantee Fund, South Korea*
[d] *NANO Co. Ltd., Chinju, South Korea*

Received 14 January 2003; received in revised form 3 April 2003; accepted 10 April 2003

Abstract

A photocatalytic-electrolysis reactor using an anode coated with a TiO_2 thin film of an anatase structure, a low surface resistivity, and a large surface area has shown an enhancement of TiO_2 photocatalytic reaction efficiency by a reduction of the recombination of photogenerated electron–hole pairs. At the photocatalytic anode under UV irradiation and with a potential to generate oxygen evolution being applied, the photocatalytic enhancement was about 90% because of suppression of the recombination of holes and electrons by taking out forcedly the generated electrons through an external bias into a cathode and by the oxygen generated by the electrolytic reaction acting as an acceptor to the electrons. The photocatalytic enhancement effect occurred only when the cell voltage applied to the photocatalytic-electrolysis reactor was over a certain value. The photocatalytic reaction observed on the catalytic oxide electrodes of RuO_2 and IrO_2 was because of the existence of TiO_2 on the electrode surface, which resulted from the oxidation of Ti substrate itself during sintering for the fabrication of the electrodes.

Keywords: Photocatalytic; Electrolysis; TiO_2; Recombination; Electron–hole

1. Introduction

TiO_2 photocatalyst has attracted a great deal of attention in environmental waste-water treatment in the past decade, because it generates highly oxidative hydroxyl radicals ($OH^{\bullet}$) which can mineralize refractory organic contaminants in water under UV irradiation, and because it has chemical stability, non-toxicity, and is low cost [1–10]. The photocatalytic TiO_2 under UV irradiation create hole–electron pairs. The holes react with hydroxyl group from water acting as electron donor to produce the hydroxyl radicals. On the other hand, the electrons react with dissolved oxygen in water acting as an electron acceptor to yield super oxide (O_2^-). Some of the generated hole–electron pairs, which do not participate in the redox reaction with water or oxygen, disappear as heat through the recombination of the holes and electrons. Therefore, the recombination of holes and electrons has been known to be one of the important factors to affect the decrease of photocatalytic efficiency. Adding an electron scavenger in TiO_2 slurry can be used to reduce the recombination. Also, a way to dope the catalytic metals or metal oxides such as Pt, RuO_2, Ag, etc., on TiO_2 particles has been studied, where the doped materials attract the electrons which result in a prohibition of the recombination of holes and electrons [8–10]. Another way to suppress the recombination effect can be considered, which pumps the photogenerated electrons through an external circuit with an electrochemical bias into a cathode. On the other hand, the catalytic oxide electrodes such as TiO_2, SnO_2, RuO_2, IrO_2, etc., called dimensionally stable anode (DSA), is known to generate the hydroxyl radicals under a potential to evolve oxygen gas, as well [11–18]. Therefore, if an electrode prepared by coating photocatalytic TiO_2 on a Ti substrate for the catalytic oxide electrode, which act as an electrolytic anode and a photocatalyst at the same time, is used as an anode of an electrolytic–photocatalytic reactor with applying a potential for oxygen evolution and irradiating UV on it, the electrode generates OH radicals by both the electrolytic and the photocatalytic reactions, as shown in Fig. 1. The photogenerated electrons on the electrode surface can be forcedly taken out into a cathode by the oxidation function of the anode, keeping the suppression of the recombination of hole–electron pairs. At that time, the

* Corresponding author.
E-mail address: nkwkim@kaeri.re.kr (K.-W. Kim).

1010-6030/$ – see front matter © 2003 Elsevier Science B.V. All rights reserved.
doi:10.1016/S1010-6030(03)00208-9

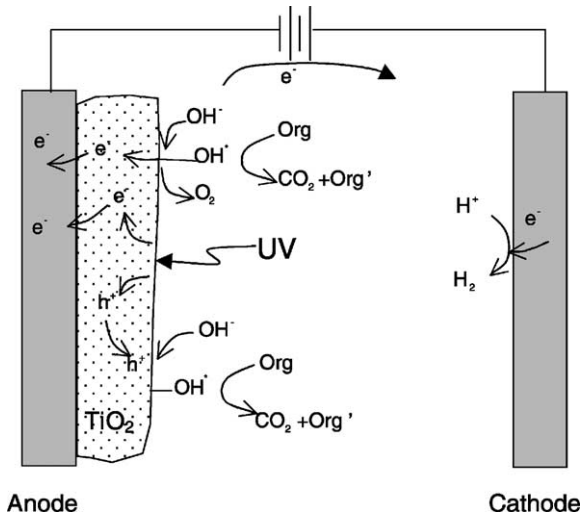

Fig. 1. Schematic photocatalytic–electrolytic reaction.

oxygen evolution occurring at the electrode increases the dissolved oxygen in a solution, which acts as an electron scavenger. Such functions by the electrolytic–photocatalytic electrode are considered to enhance the photocatalytic efficiency by an inhibition of the recombination of holes and electrons. The electrolytic–photocatalytic electrode needs material properties to operate at a low overpotential for the oxygen evolution and to have a good electric contact between the electrode substrate and the TiO_2 coating layer on it so that the generated electrons may be transported easily to an external circuit.

In this work, the TiO_2 electrode to be used as an anode of an electrolytic–photocatalytic reactor was fabricated, and an enhancement effect of photocatalytic reaction efficiency was investigated by using the electrode. Also the electrolytic–photocatalytic characteristics of RuO_2 and IrO_2 electrodes were compared with that of the TiO_2 electrode.

2. Experimental

A schematic diagram of an experimental apparatus used in this work was shown in Fig. 2. A 450 W mercury vapor UV lamp (Hanovia) was used for the photocatalytic reaction, and a Vycor adsorption sleeve to cut off the wavelengths less than 250 nm was placed between the lamp and a quartz immersion well (Ace glass) inside which the lamp was put. The quartz immersion well kept at $25 \pm 0.5\,^{\circ}C$ by circulating coolant from a chiller was inserted into the center of an acryl reactor of 9.5 cm in diameter and 30 cm in length. An annual anode coated with TiO_2 for the electrolytic–photocatalytic reaction and an annual cathode with a distance of 5 mm were installed between the quartz immersion well and the inside of the acryl reactor. The current applied between the anode and the cathode was controlled with a potentiostat (Wonatech, WMPG1000HP). A solution of 2000 ml was circulated inside the reactor with a pump and an external reservoir. The solution was prepared by dissolving 4CP of 50 ppm in 0.2 M $NaNO_3$ which helped the solution to have some conductivity for the electrolysis reaction. For the organic destruction test, the solution was sampled at regular intervals and then its total organic carbon was measured with a TOC analyzer (Shimadzu TOC-5000A).

A substrate for the electrolytic–photocatalytic anode to be coated with a photocatalytic oxide of TiO_2, RuO_2, and

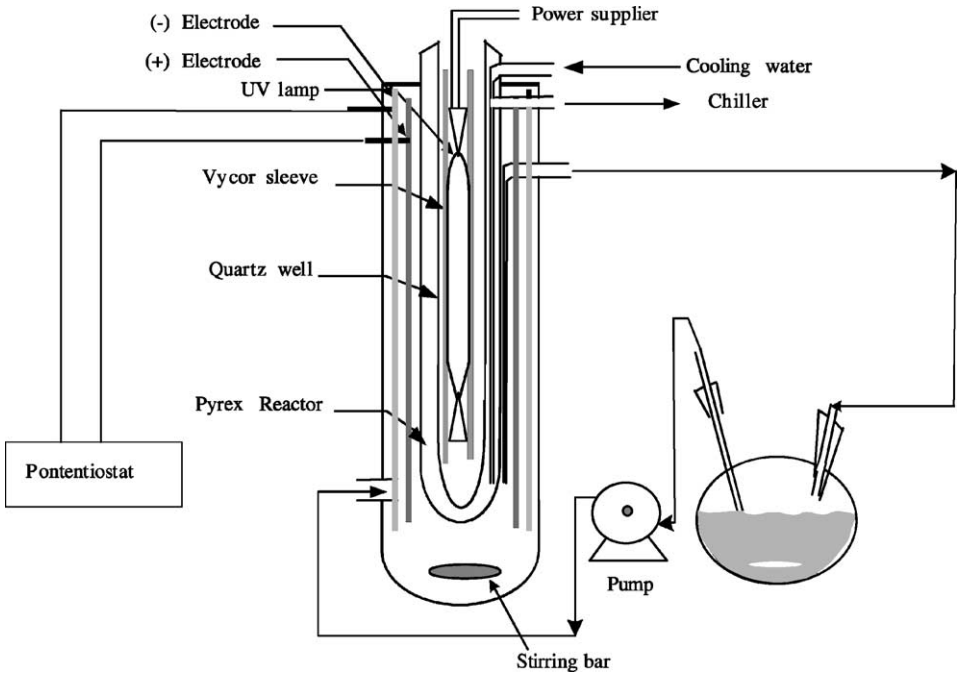

Fig. 2. Experimental apparatus for a photocatalytic–electrolytic reactor.

IrO_2 is a Madras type Ti of 6.5 cm in diameter and 29 cm in length with a mesh of 6 mm × 3 mm. The same Ti substrate with a 7.5 cm diameter was directly used for a cathode of the electrolytic–photocatalytic reactor. For fabrication of the anode, the Ti substrate was first etched in 35% HCl at 61 ± 1 °C for 1 h. A way for coating TiO_2, RuO_2, and IrO_2 on the etched Ti substrate was the same as that used in our previous papers to fabricate some catalytic oxide electrodes [17–19]. The etched Ti substrate following washing and drying was dipped into the precursor solutions of $TiCl_3$, $TiCl_4$, $IrCl_3$, and $RuCl_3$ (0.2 M dissolved in 1:1 v/o HCl). It was dried at 90 °C for 5 min, sintered at 350 °C for 10 min. These steps were repeated to get multiple coating layers, and then it was finally annealed between 400 and 700 °C for 1 h.

Material properties of the electrode were evaluated by XRD and XPS (X-ray photoelectron spectroscopy: VG scientific ESCALB-200R). The surface resistivity of the oxide electrode was simply measured by a multi-meter with two probes of a constant distance as an average value of 10 measurements.

3. Results and discussion

Because the TiO_2 electrode as an anode of the electrolytic–photocatalytic reactor to be used for the purpose of this work needs a good electronic contact not only between the TiO_2 coating and the substrate but also between all the particles constituting the coating on the substrate surface, the TiO_2 photocatalytic layer on the Ti substrate was prepared by sintering the Ti substrate painted with a precursor solution of titanium chloride rather than by the usual way to fix TiO_2 particles on some substrates with an organic binder. If an organic binder is used in our work, it can hinder the electron transfer through the Ti substrate to an external circuit. And it can reduce the photocatalytic activity of the TiO_2 by coating the TiO_2 particle surfaces with the binder. Also the binder itself could be degraded by the photocatalytic reaction. In an immobilized TiO_2 system, it is very important that the system has a large photo-active surface area to contact the TiO_2 with a target solution as much as possible. And an initial surface condition of the Ti substrate to be used for the fabrication of the TiO_2 electrode has a great effect on several properties of the final product after sintering such as morphology, roughness, cohesion of the oxide coating (anchoring effect), and so on. They subsequently affect the application of the electrode in view of electrode activity and lifetime [14,17,18]. Therefore, first of all, the Ti substrate was etched in 35% HCl at 61 ± 1 °C for 1 h so that the surface may have lots of roughness before the substrate was painted with a precursor solution. Fig. 3 shows the SEM micrographs of the Ti substrate before and after etching. The etched substrate had a sharp ripple surface with fine roughness without the initial grain boundary shape before etching. The etching depths were about 8–9 μm, and the weight loss of Ti substrate was about 1.34 wt.% (7.08 mg/cm^2 h). The Ti surface after HCl etching became dark gray due to titanium hydride (TiH_2) formed during etching, which was confirmed by other works [17,20–22].

In view of the photodegradation of various pollutants, anatase structure of TiO_2 is known to be in general much higher than that of rutile [10,23]. The etched substrate is Ti metal, so there is a possibility that the substrate could have anatase TiO_2 on its surface by sintering it simply at a temperature. In order to confirm it, the etched Ti substrates were sintered at a range of 300–800 °C and their XRD results are shown in Fig. 4. Under 400 °C, TiO_2 was not significantly formed, but TiO_2 of rutile started to form apparently over 500 °C, and then the substrate was completely covered with TiO_2 of rutile over 700 °C. From this result, it is considered that the direct sintering of the Ti substrate itself cannot form the anatase phase on its surface. Accordingly, sintering of the etched Ti substrates painted with $TiCl_3$ or $TiCl_4$ precursor solution was tried to obtain the anatase structure. Before doing it, the $TiCl_3$ and $TiCl_4$ precursor solutions themselves were sintered at 500 and 700 °C and their XRD results are shown in Fig. 5. In the case of $TiCl_4$, complete anatase was formed at both 500 and 700 °C. In the case of $TiCl_3$, a

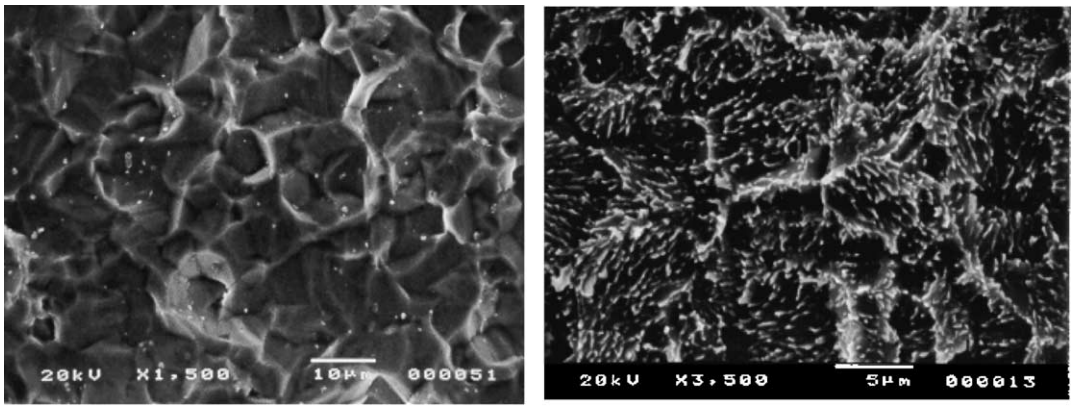

(a) Ti substrate before etching

(b) After etching in 35% HCl at 62°C for 1hr

Fig. 3. SEM micrographs of the Ti substrate before and after etching.

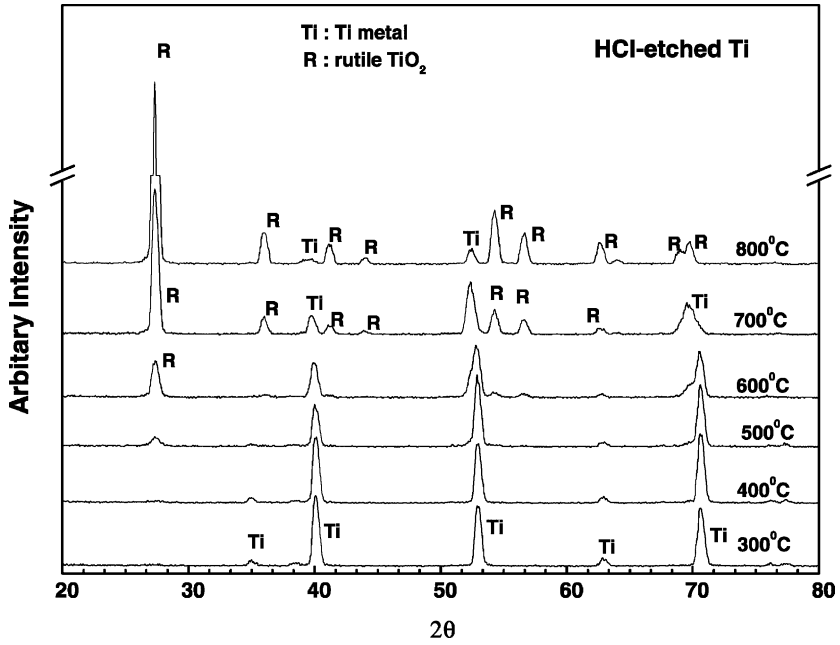

Fig. 4. XRD patterns after sintering the etched Ti substrates with sintering temperature.

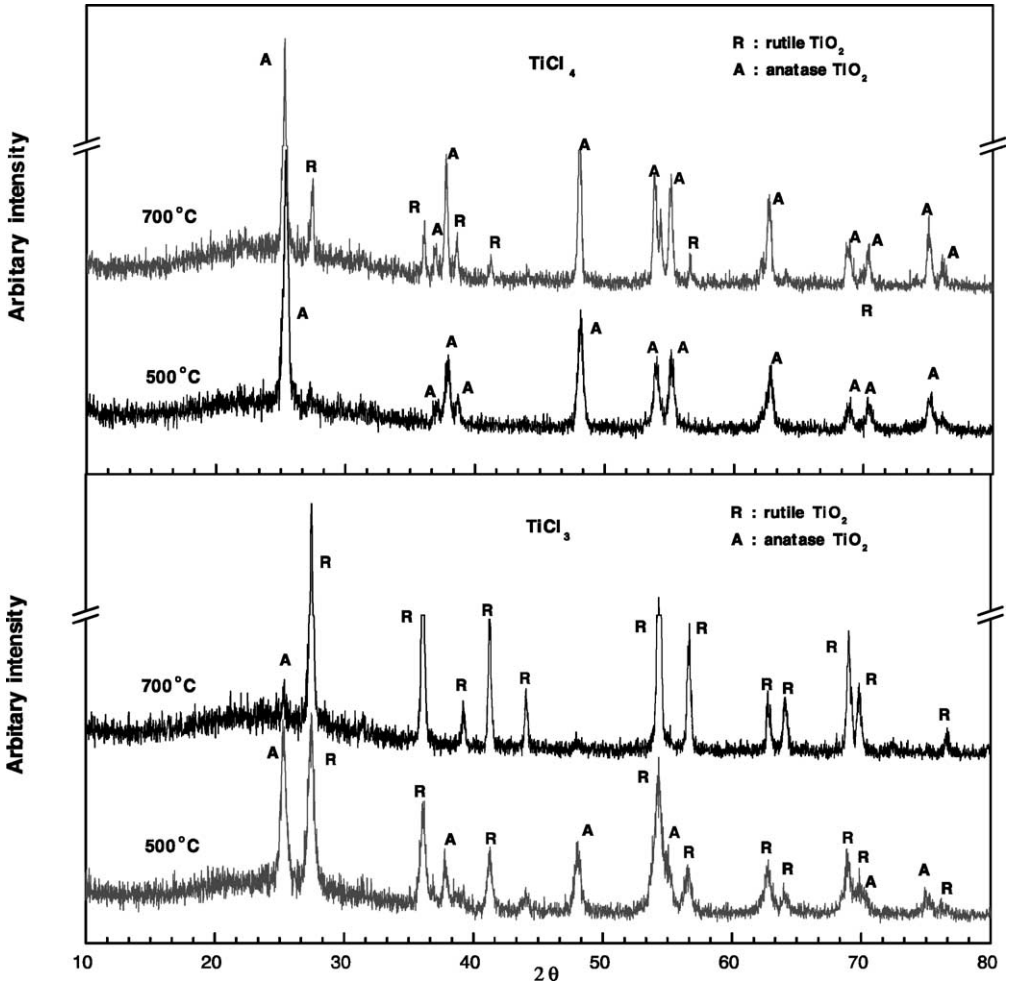

Fig. 5. XRD patterns after sintering the etched Ti substrates with $TiCl_4$ coating with sintering temperature.

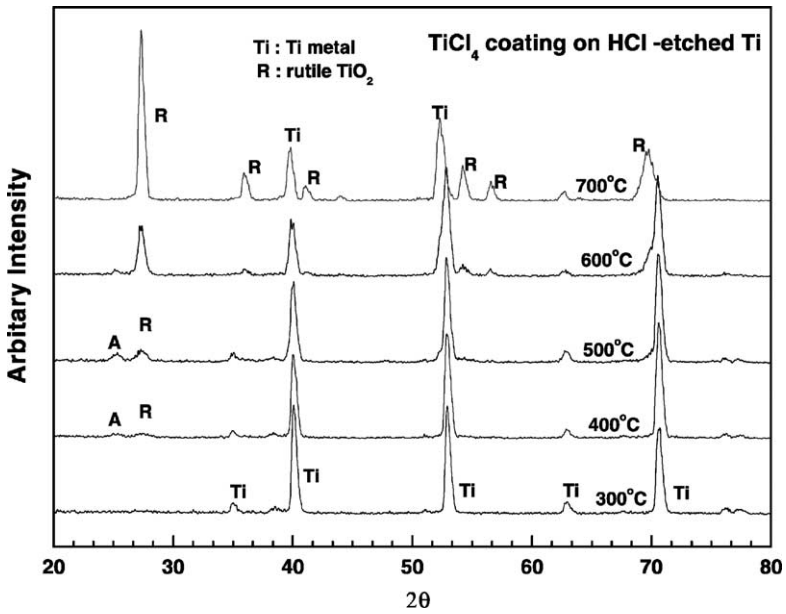

Fig. 6. XRD patterns after sintering the etched Ti substrates with $TiCl_4$ coating with sintering temperature.

composite structure of anatase and rutile were formed at 500 °C, however, the anatase phase was converted to the rutile phase at 700 °C. Figs. 6 and 7 show the XRD results after sintering the etched Ti substrates painted with $TiCl_3$ and $TiCl_4$ precursor solutions at a range of 300–700 °C. Being different from the result of Fig. 5, both cases of the sintered Ti substrates painted with $TiCl_3$ and $TiCl_4$ precursor solutions show composite TiO_2 structures of rutile and anatase only at a range of about 400–600 °C. The anatase structure disappears over 600 °C and only the rutile structure remains. The anatase portion of the case of Ti substrate coated with $TiCl_3$ is observed to be higher than that of the case of Ti substrate coated with $TiCl_4$, even though the difference is small. The difference between the results of Figs. 5–7 is considered to be due to the difference in thermal decomposition mechanisms of $TiCl_3$ and $TiCl_4$ directly to TiO_2 and those of them to TiO_2 on the etched Ti substrate with TiH_2 on its surface.

When an electrode with anatase TiO_2 coating for the photocatalytic reaction is used as an anode for an electrolytic reaction at the same time, it needs to have a low surface resistivity, which makes the electrode operate at a low potential

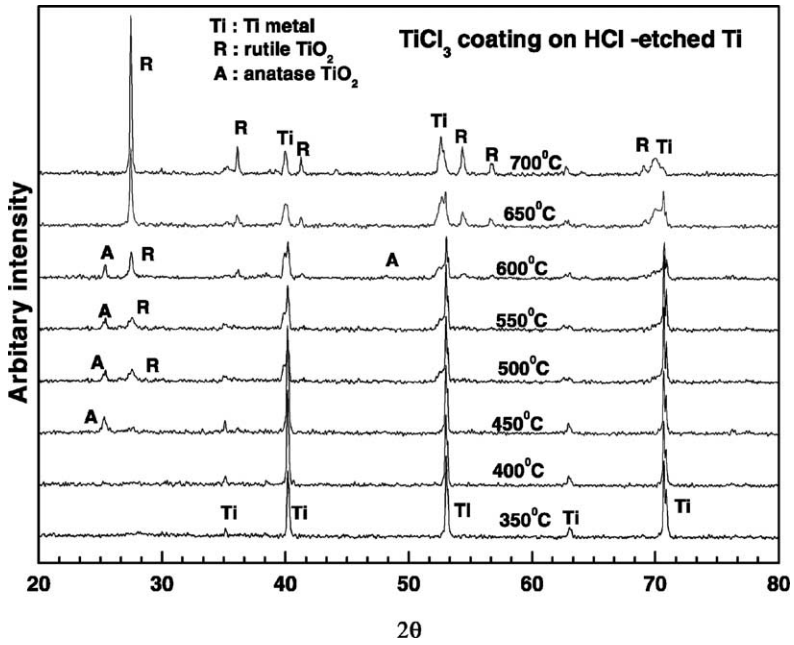

Fig. 7. XRD patterns after sintering the etched Ti substrates with $TiCl_3$ coating with sintering temperature.

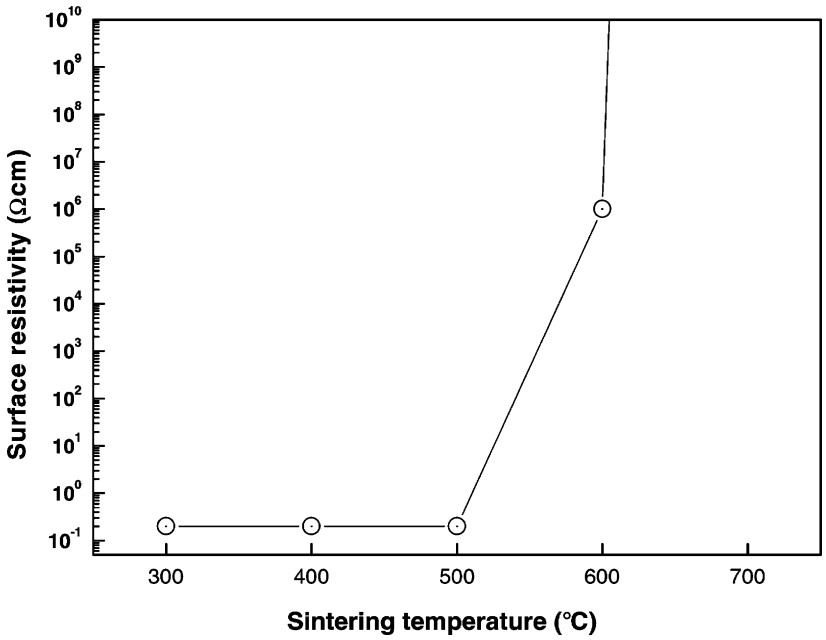

Fig. 8. Surface resistivities of the Ti substrates with sintering temperature.

when a controlled current is applied to the electrode. The surface resistivities after sintering the etched Ti substrates with temperature were measured and the results are shown in Fig. 8. The surface resistivity remains under about 1 Ω cm at less than 550 °C, but goes up rapidly after 550 °C so that it comes to about 1000 Ω cm at 700 °C. Non-stoichiometric titanium oxides of TiO_x, are known to have high electric conductivities in a range of $1.5 < x < 2$ [11]. And the photocatalytic TiO_2 is known to have some defective structures due to oxygen vacancy which is effective for the adsorption of hydroxyl groups to be converted to hydroxyl radical, i.e., it exists in a form of TiO_x [10,24–27]. Similarly, a catalytic metal oxide electrode for the generation of the hydroxyl radicals under an oxygen evolution potential is known to have a chemical non-stoichiometric oxide form, i.e. MO_x, $0 < x < 2$ on its surface [17,28–30]. Therefore, in view of these facts and results of Figs. 6 and 7, the TiO_2 electrode for a electrolytic–photocatalytic reactor fabricated by sintering an etched Ti substrate coated with a $TiCl_3$ precursor solution at about 500 °C is considered to have some non-stoichiometric oxide on its surface which makes the electrode have a low surface resistivity and a photocatalytic property.

Fig. 9 shows the removal yields of TOC of 4CP by an etched Ti substrate itself, a TiO_2 electrode of only rutile phase sintered at 700 °C, and a TiO_2 electrode of a composite phase of rutile and anatase sintered at 500 °C under only UV irradiation without applying current. The TOC removal yields by the Ti substrate without the TiO_2 coating is about 5%, which is considered to be almost due to the decomposition by UV, because the TOC removal yield by irradiating UV in a solution without the etched Ti substrate was about 3–4%. The TOC removal yields by the TiO_2 electrodes with rutile phase and a composite phase of rutile and anatase are about 7 and 15%, respectively. These results confirm again that TiO_2 of anatase has better photocatalytic activity than that of rutile. Fig. 10 shows the TOC removal yields by only electrolytic reaction using the TiO_2 anode with an anatase composition and by the electrolytic–photocatalytic reaction using the same electrode under UV irradiation with a change of current density. The TOC removal yield by the UV photocatalytic reaction was 15%. Until a current density of 0.7 mA/cm^2, the TOC removal yields by the electrolytic–photocatalytic reaction agree well with the summations of the TOC removals by respective electrolytic and photocatalytic reactions, which were carried out independently. However, over the current density, the TOC removal yields by the electrolytic–photocatalytic reaction are higher by a certain value than the summations of those of the respective electrolytic and photocatalytic reactions. The deviation is considered to occur from an enhanced photocatalytic reaction. In other words, it can be explained by the following two reasons. The first one is that the photogenerated electrons on the anode surface under UV irradiation were forcedly taken out into a cathode by an external bias of potentiostat, resulting in a suppression of the recombination of the hole–electron pairs. The similar improvement of degradation of 4CP in a photoelectrochemical system using TiO_2 thin film prepared by a chemical vapor deposition method was observed in a previous paper [33]. However, in that system, the TiO_2 film did not act as a catalytic oxide electrode to generate the hydroxyl radicals under a potential to evolve oxygen gas. The second one is because of the oxygen evolution occurring at the electrode, which acts as an electron scavenger in solution. Fig. 11 shows the photocatalytic

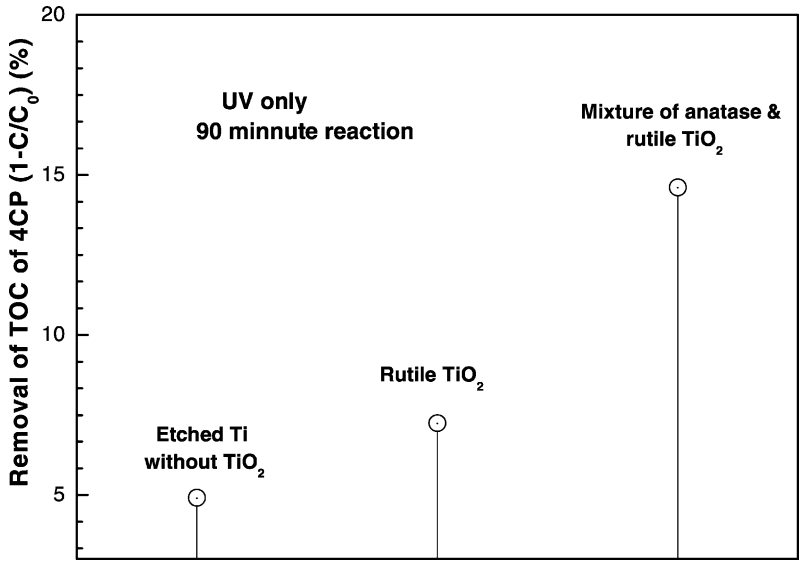

Fig. 9. Removal yields of TOC of 4CP by TiO_2-coated anodes under UV irradiation without electrolysis.

enhancement defined as a [(TOC removal by an electrolytic–photocatalytic reaction) − (TOC removal by an electrolytic reaction) − (TOC removal by a photocatalytic reaction)]/(TOC removal by a photocatalytic reaction) × 100 on the basis of the results of Fig. 10 and it also shows the voltages between anode and cathode at the applied current densities of Fig. 10, i.e. showing an *i–V* relation of the electrolytic–photocatalytic cell. The photocatalytic enhancement is almost constantly 90% at more than 0.7 mA/cm^2. The photocatalytic enhancement effect is observed to occur only from a minimum cell voltage of more than 12 V. The cell voltage is considered to involve an overpotential required to overcome the Schcottky barrier between the metal Ti substrate and TiO_2 coating layer where the electron trapping occurs [10] and to overcome a voltage drop when the electrons pass a contacting layer between the Ti substrate and the TiO_2 coating into a cathode.

Fig. 12 shows the TOC removal yields by an electrolytic–photocatalytic reaction using RuO_2 and IrO_2 electrodes which were prepared in the same way as the TiO_2 electrode, being compared with those by TiO_2 electrode. The TOC removal yields only by the electrolytic reaction using the RuO_2 and IrO_2 electrodes are 39 and 18%, respectively. That by the RuO_2 electrode is about two times higher than that by the IrO_2 electrode. This agrees with our previous results [18,19]. The TOC removal yields only by irradiating

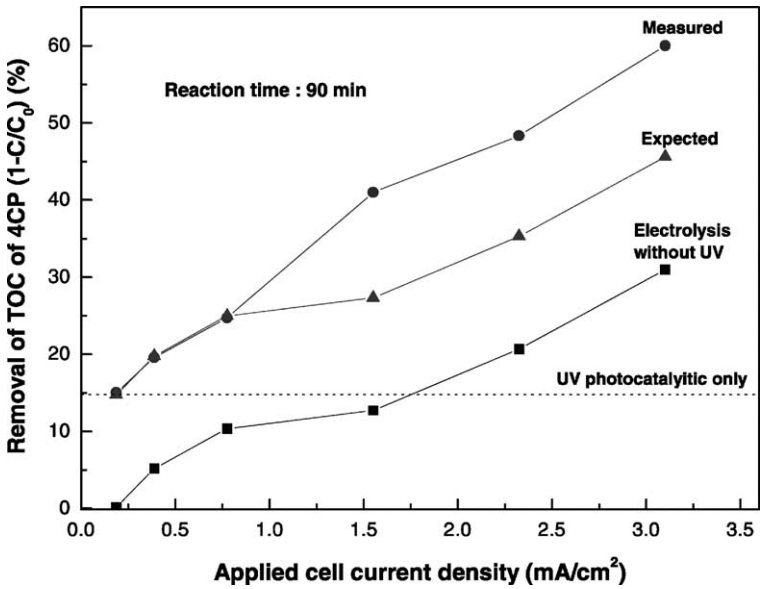

Fig. 10. Removal yield of TOC of 4CP by TiO_2-coated anode under UV irradiation and electrolysis with applied cell current density.

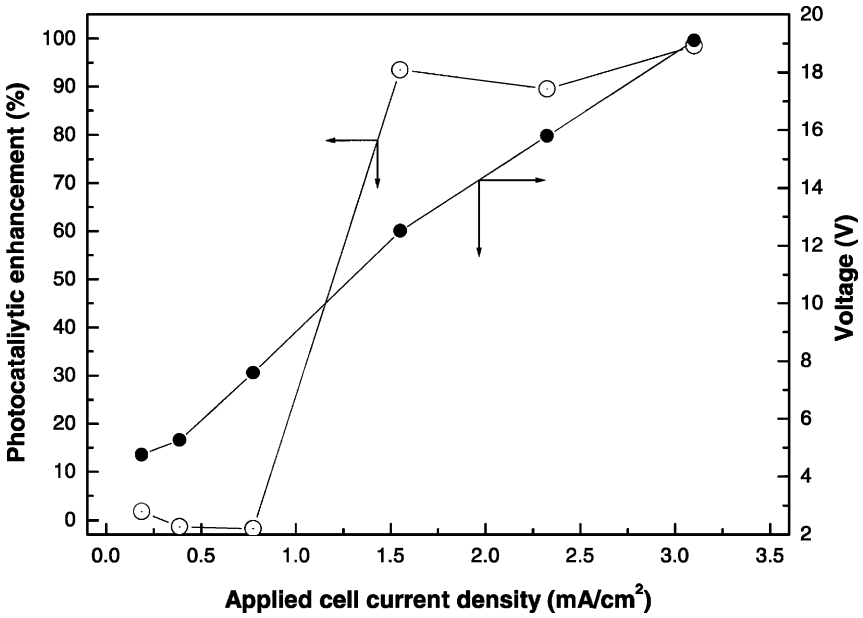

Fig. 11. Photocatalytic enhancement and cell voltage with applied cell current density.

UV on RuO_2 and IrO_2 electrodes without applying current are 22 and 15%, respectively. The TOC decomposition is considered to be due to a photocatalytic reaction of the TiO_2 existing on the electrodes rather than due to those of RuO_2 and IrO_2 themselves. When the $IrCl_3$ or $RuCl_3$-coated Ti substrate is sintered at a high temperature, an oxidation of Ti substrate itself occurs and the formed titanium oxide solid-diffuses up to the surface, which results in the coexistence of TiO_2 and RuO_2 (or IrO_2) on the surface [17,18,31,32]. To confirm it, an XPS spectrum of IrO_2 electrode prepared at 570 °C was measured, as shown in Fig. 13. The peak of Ti $2p_{3/2}$ due to the solid diffusion of TiO_2 from the Ti substrate to the electrode surface as well as the peaks of Ir of 4p, 4d, 4f are observed to be well developed. The same phenomenon is considered to happen at the RuO_2 electrode. The photocatalytic enhancements in the electrolytic–photocatalytic reaction using RuO_2 and IrO_2 anodes calculated on the basis of results of Fig. 12 were about 80 and 120%, respectively, as shown in Fig. 14.

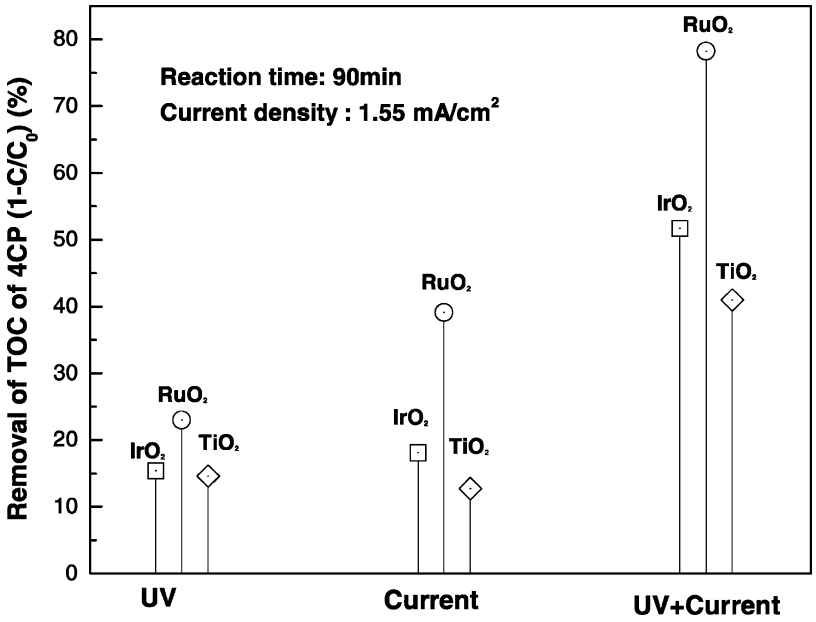

Fig. 12. Removal yields of TOC of 4CP by IrO_2, RuO_2 and TiO_2 anodes under UV irradiation with electrolysis.

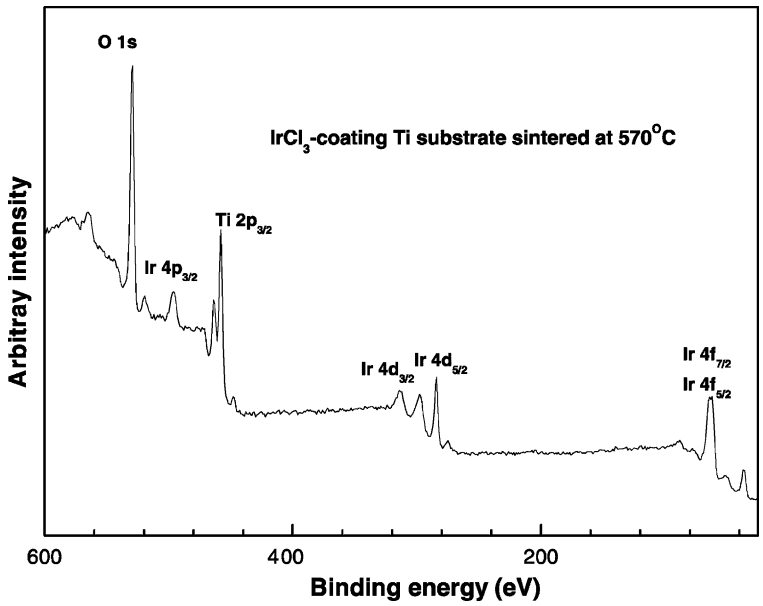

Fig. 13. XPS spectrum of $IrCl_3$-coated Ti substrate sintered at 570 °C for 1 h.

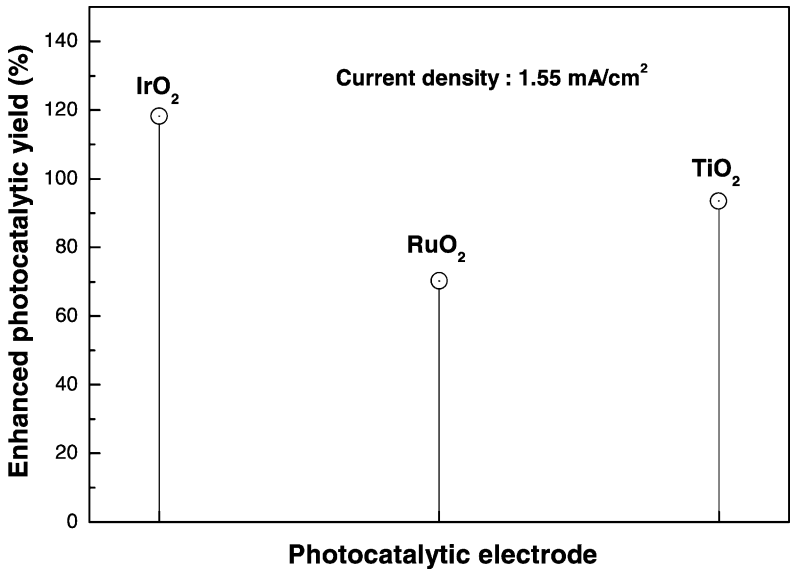

Fig. 14. Photocatalytic enhancements by IrO_2, RuO_2 and TiO_2 anodes under UV irradiation with electrolysis.

4. Conclusion

The electrode prepared by a HCl-etched and $TiCl_3$-painted Ti substrate sintered at about 500 °C had a low surface resistivity, a large surface area, and anatase TiO_2 coating on its surface so that it could be used as an anode of an electrolytic–photocatalytic reactor. The photocatalytic reaction efficiency was enhanced by about 90% by suppressing the recombination of the hole–electron pairs in the electrolytic–photocatalytic reactor. The photocatalytic enhancement occurred only when the applied cell voltage exceeded a certain value. The photocatalytic reactions of IrO_2 and RuO_2 electrodes was by the TiO_2 existing on the electrode surface, which was due to the oxidation of the Ti substrate itself and its solid diffusion to the surface during the sintering.

Acknowledgements

This work was supported by Ministry of Commerce, Industry and Energy in South Korea.

References

[1] A. Fusjishima, K. Honda, Nature 238 (1971) 3.
[2] B. Kraeutler, A.J. Bard, J. Am. Chem. Soc. 100 (1977) 598.
[3] D.F. Ollis, A.L. Pruden, J. Catal. 82 (1983) 40.
[4] R.W. Matthews, J. Chem. Soc., Faraday Trans. 80 (1984) 45.
[5] J. Sabate, M.A. Anderson, J. Catal. 27 (1991) 16.
[6] L.P. Childs, D.F. Ollis, J. Catal. 67 (1981) 3.
[7] N. Djeghri, S.T. Teichner, J. Catal. 62 (1980) 9.
[8] M. Litter, Appl. Catal. B 23 (1999) 8.
[9] A. Hagfeldt, M. Gratzel, Chem. Rev. 95 (1995) 4.
[10] A.L. Linsebigler, G. Lu, J.T. Yates Jr., Chem. Rev. 95 (1995) 73.
[11] K. Rajeshwar, J.G. Ibanez, Environmental Electrochemistry, Academic press Inc., London, 1997.
[12] K. Scott, Electrochemical Process for Clean Technology, The Royal Society of Chemistry, UK, 1995.
[13] K. Kinoshida, Electrochemical Oxygen Technology, Wiley, New York, 1992.
[14] S. Trasatti, Electrode of Conductive Metallic Oxides, Part A, Elsevier, Amsterdam, 1980.
[15] S. Trasatti, Electrochim. Acta 29 (11) (1984) 1504.
[16] C. Comniellis, Electrochim. Acta 39 (11/12) (1994) 1857.
[17] K.-W. Kim, E.-H. Lee, J.S. Kim, K.H. Shin, K.H. Kim, Electrochim. Acta 46 (2001) 915.
[18] K.-W. Kim, E.-H. Lee, J.S. Kim, K.H. Shin, B.I. Chung, Electrochim. Acta 47 (2002) 2525.
[19] K.W. Kim, E.H. Lee, J.-S. Kim, K.-H. Shin, B.-I. Chung, J. Electrochem. Soc. 149 (2002) D187.
[20] L.D. Silva, V.A. Alves, M.A.P.D. Silva, S. Trasatti, J.F.C. Boots, Can. J. Chem. 75 (1997) 1483.
[21] J. Krysa, L. Kule, R. Mraz, I. Rousar, J. Appl. Electrochem. 26 (1996) 999.
[22] J. Krysa, R. Mraz, Electrochim. Acta 40 (12) (1995) 1997.
[23] K.S. Jung, H.I. Lee, J. Korean Chem. Soc. 41 (21) (1997) 682.
[24] R.L. Kurtz, R. Stockbauer, T.E. Madey, Surf. Sci. 218 (1989) 178.
[25] S. Bourgeois, F. Jomard, M. Perdereau, Surf. Sci. 279 (1992) 349.
[26] P.B. Smith, S.L. Bernasek, Surf. Sci. 188 (1987) 241.
[27] K.-W. Kim, E.-H. Lee, Y.-J. Kim, M.-H. Lee, K.-H. Kim, D.-W. Shin, J. Photochem. Photobiol. A: Chemistry 159 (2003) 299.
[28] D. Galizzioli, F. Tantardini, S. Trasatti, J. Appl. Electrochem. 5 (1975) 203.
[29] D. Galizzioli, F. Tantardini, S. Trasatti, J. Appl. Electrochem. 4 (1974) 57.
[30] R.S. Teo, J. Orehotsky, W. Visscher, S. Srinivasan, J. Electrochem. Soc. 128 (9) (1981) 1900.
[31] C. Angelinetta, S. Trasatti, Mater. Chem. Phys. 22 (1989) 231.
[32] A.D. Battisti, R. Brina, G. Gaveeli, A. Benedetti, G. Fagherazzi, J. Electroanal. Chem. 200 (1985) 93.
[33] M. Hitchman, F. Tian, J. Electroanal. Chem. 538 (2002) 165.